Aspect Independent Spherical Target Recognition Using Structural Features of Scattered Signals

M. Alper SELVER, E. Yeşim ZORAL and Suat DORAK
Dokuz Eylül University, Engineering Faculty, Electrical and Electronics Engineering Department
Tınaztepe Kampüsü, Buca, 35160, Izmir, Turkey
alper.selver@deu.edu.tr

***Abstract*— The classification of similar targets from scattered electromagnetic signals is a challenging problem due to the strong dependency to aspect angle. In order to classify a target effectively, distinguishable features should be extracted and adequately processed to gain independency from the adverse effects of aspect angle. In this study, an electromagnetic target classification method for spherical targets under strong noise is proposed. First, a novel feature set, which can be extracted directly from scattered time domain signals, is introduced. Next, it is shown that this novel feature set carries aspect independent representation of the targets by analysis of the principle components. Finally, cross validation learning strategy is used for evaluation of the proposed feature set. The results show that, up to -20 dB SNR, perfectly conducting spherical targets can effectively be recognized.**

***Index Terms*— Radar, Feature Extraction, Classification.**

I. Introduction

Target recognition from the back-scattered signals of similar targets is a challenging task [1-3] even for targets with simple geometry due to complicated scattering mechanisms one of which is aspect angle dependency.

II. Generation of Scattered Signals

The scattered electric fields can be expressed in terms of Hertz and Debye potentials as in [2]. In this study, target responses are numerically synthesized with these expressions for a plane wave excitation which is linearly polarized in x-direction and propagates in z-direction (Figure 1).

The far field scattered responses are computed using MATLAB 7.1 in frequency domain over a bandwidth from zero to 12 GHz at 873 frequency sample points with frequency resolution of 13.75 MHz which can be regarded as resonance region. These responses are also obtained at $\varphi = \pi/2$ plane, with a radial distance of 72 cm from the sphere center, for twelve different Bistatic Aspect Angles (BAA), 180- $\theta = \theta_b$ = 10, 20, … 180 degrees in Figure 1.

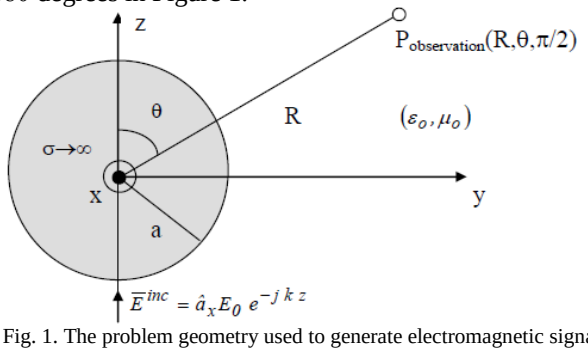

Fig. 1. The problem geometry used to generate electromagnetic signals scattered from the spherical targets

After getting frequency responses, time-domain scattered fields are computed by using Gaussian windowing, inverse fast Fourier transformation (IFFT) and zero padding to get a 5 ps resolution, which is enough to observe the frequency range up to 12 GHz. The resulting time signals have 1024 sample points with a total time span of 5.115 ns (Figures 2 and 3).

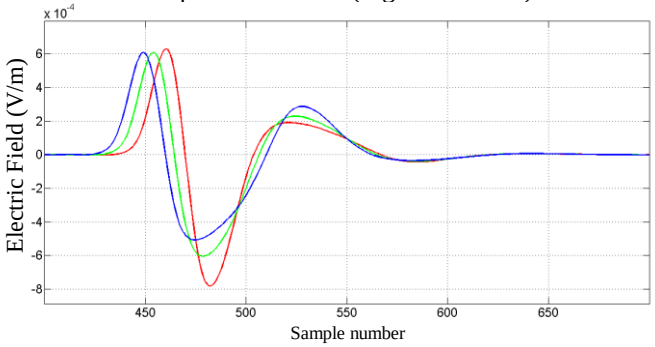

Fig. 2. The scattered time domain signals for the conducting sphere of radius 2.4 cm at the bistatic aspect angles of 60° (red), 90° (green) and 120° (blue) .

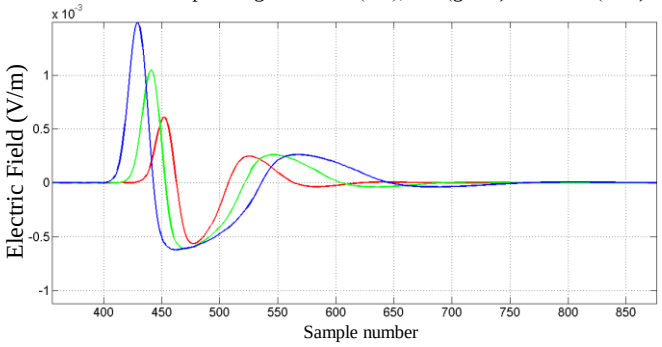

Fig. 3. The scattered time domain signals for the conducting sphere of radius 2.4cm (red), 3.6cm (green) and 4.8cm (blue) at bistatic aspect angle of 100°.

The noisy scattered time domain signals at all the aspect angles stated above are synthesized at the signal-to noise ratio (SNR) levels of 20, 10, 0 and -20 dB to be used for classifier design and for performance testing.

III. Structural Feature Extraction and Processing

Typical scattered signals in Figure 2 and Figure 3 show that these signals can be divided into four sub-waves. Analysis of these sub-waves shows that the amplitude and duration of these 4 sub-waves differ depending on the radius of the target. Thus, if aspect angle effects can be eliminated, these sub-wave properties (i.e. structural features) can be used to classify similar spheres with different radii.

The peaks and durations of these four sub-waves constitute a structural feature set for the corresponding scattered signal (Figure 4). For instance, the peak value of the first wave is

named as FPA (First Peak Amplitude) and the duration between the first zero crossing prior to FPA and FPA is named as FWLH (First Wave Left Half). Similarly, the duration between the first zero crossing after FPA and FPA is named as FWRH (First Wave Right Half). If a similar strategy is used to extract corresponding structural features for the remaining three sub-waves shown in Figure 4, SPA (Second Peak Amplitude), SWLH (Second Wave Left Half), SWRH (Second Wave Right Half); TPA (Third Peak Amplitude), TWLH (Third Wave Left Half), TWRH (Third Wave Right Half); QPA (Quartus Peak Amplitude) QWLH (Quartus Wave Left Half), QWRH (Quartus Wave Right Half), can be obtained.

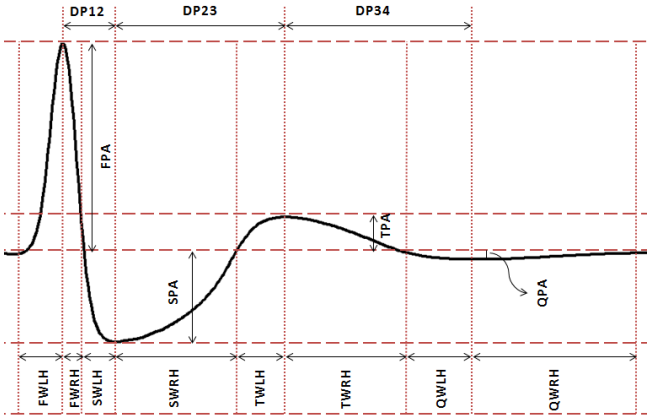

Fig. 4. Extraction of the proposed features from a scattered signal

Moreover, DP12 (Duration between peaks 1-2), DP23 (Duration between peaks 2-3); DP34 (Duration between peaks 3-4) that represent peak occurrence timings are computed. Finally, using the above introduced structural features, which are obtained directly from the signal, is concatenated with slope features representing how fast a peak occur after a zero crossing and how fast a peak drops to zero. (These features are named as: FWLS=FPA/FWLH (First Wave Left Slope), FWRS=FPA/FWRH (First Wave Right Slope) and similarly SWLS=SPA/SWLH, SWRS=SPA/SWRH, TWLS=TPA/TWLH, TWRS=TPA/TWRH QWLS=QPA/QWLH, QWRS=QPA/QWRH).

The extraction of above mentioned 23 features for 18 BAA results with a 441 dimensional feature space for each sphere. The dependency of extracted features to sphere radius and BAA is controlled using the analysis of principle components [3]. Application of analysis generated 7 uncorrelated principle components with contributions 93.0765%, 2.42%, 1.74%, 1.08%, 0.82%, 0.58%, 0.28%. In depth analysis of these components also show that the modified feature space is not dependent to aspect angle in representing spherical targets since they become linearly separable (Figure 5).

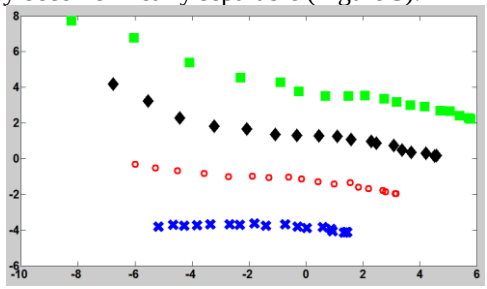
Fig. 4. Feature space after PCA

IV. Performance Evaluation and Results

In this study, classification of 4 spherical targets (i.e. radii: 1.8cm, 2.4cm, 3.0cm, and 3.6cm) is simulated. Feature vectors extracted for each sphere for 18 BAA generates 18x4=72 samples for training and testing. Due to this small sample set, a K-fold partition of the data set is created [5]. For each of K experiments, K-1 folds are used for training and the remaining fold for testing. The advantage of K-fold cross validation is that it prevents over-fitting by systematically using all the examples in the data set are for both training and testing. Extensive experimentation shows that K=9 provides best results (Tables 1, 2 and 3).

TABLE I
ACCURACY (CORRECT CLASSIFICATION) PERFORMANCE

Accuracy (%)	Sphere 1	Sphere 2	Sphere 3	Sphere 4
SNR=∞	99.54	99.63	99.82	99.63
SNR=20 dB	99.07	98.89	99.58	99.86
SNR=10 dB	98.94	99.03	98.98	99.91
SNR= 0 dB	97.77	96.01	97.63	99.49
SNR=-20 dB	95.69	85.46	87.50	99.68

TABLE II
SELECTIVITY PERFORMANCE

Accuracy (%)	Sphere 1	Sphere 2	Sphere 3	Sphere 4
SNR=∞	98.33	99.26	99.81	99.54
SNR=20 dB	98.30	99.26	99.63	99.86
SNR=10 dB	98.15	98.70	98.43	99.50
SNR= 0 dB	96.67	91.11	97.03	98.67
SNR=-20 dB	94.63	76.67	82.69	98.17

TABLE III
SENSITIVITY PERFORMANCE

Accuracy (%)	Sphere 1	Sphere 2	Sphere 3	Sphere 4
SNR=∞	99.94	99.75	99.81	99.63
SNR=20 dB	99.94	98.77	99.53	99.86
SNR=10 dB	99.20	99.14	99.54	99.91
SNR= 0 dB	98.14	97.65	98.24	99.49
SNR=-20 dB	96.05	88.40	92.31	99.68

V. Discussions

The results show very high performance on classification of spherical targets by eliminating diverse effect of aspect angle dependency. Moreover, the above mentioned results are obtained for the folds that are ordered according to aspect angle (i.e. hardest case due to high difference BAA). Application of the same strategy in Section IV to randomly generated folds result with almost 100% performance. These results show the potential of the proposed novel feature set in further applications including dielectric targets.

References

[1] F. Henrotte and K. Hameyer, "The structure of EM energy flows in continuous media," *IEEE Trans. on Magn.*, vol.42, no.4, pp. 903-906,

[2] M., Secmen, G., Turhan-Sayan, "Radar target classification method with reduced aspect dependency and improved noise performance using MUSIC algorithm," *IET Radar, Sonar and Navig*.,3(6), 583–595, 2009.

[3] G., Turhan-Sayan, "Real Time Electromagnetic Target Classification Using a Novel Feature Extraction Technique with PCA-Based Fusion," *IEEE Trans. on Antennas and Prop*., Vol.53, No.2,766-776, 2005.

[4] S.J. Raudys, A. K. Jain, "Small sample size effects in statistical pattern recognition" *IEEE Trans. on Pattern Analysis and Machine Intelligence*, vol. 13, no. 3, pp. 252-264, Mar. 1991.